Supporting Information

Iron Oxide @ Polypyrrole Nanoparticles as a Multifunctional Drug Carrier for Remotely Controlled Cancer Therapy with Synergistic Anti-Tumor Effect

*Chao Wang[1]‡, Huan Xu[1]‡, Chao Liang[1], Yumeng Liu[2], Zhiwei Li[1], Guangbao Yang[1], Liang Cheng[1], Yonggang Li[2], Zhuang Liu[1]**

[1]Jiangsu Key Laboratory for Carbon-Based Functional Materials & Devices, Institute of Functional Nano & Soft Materials (FUNSOM), Soochow University, Suzhou, Jiangsu 215123, China and [2]Department of Radiology the First Affiliated Hospital of Soochow University Suzhou, Jiangsu, 215006, China

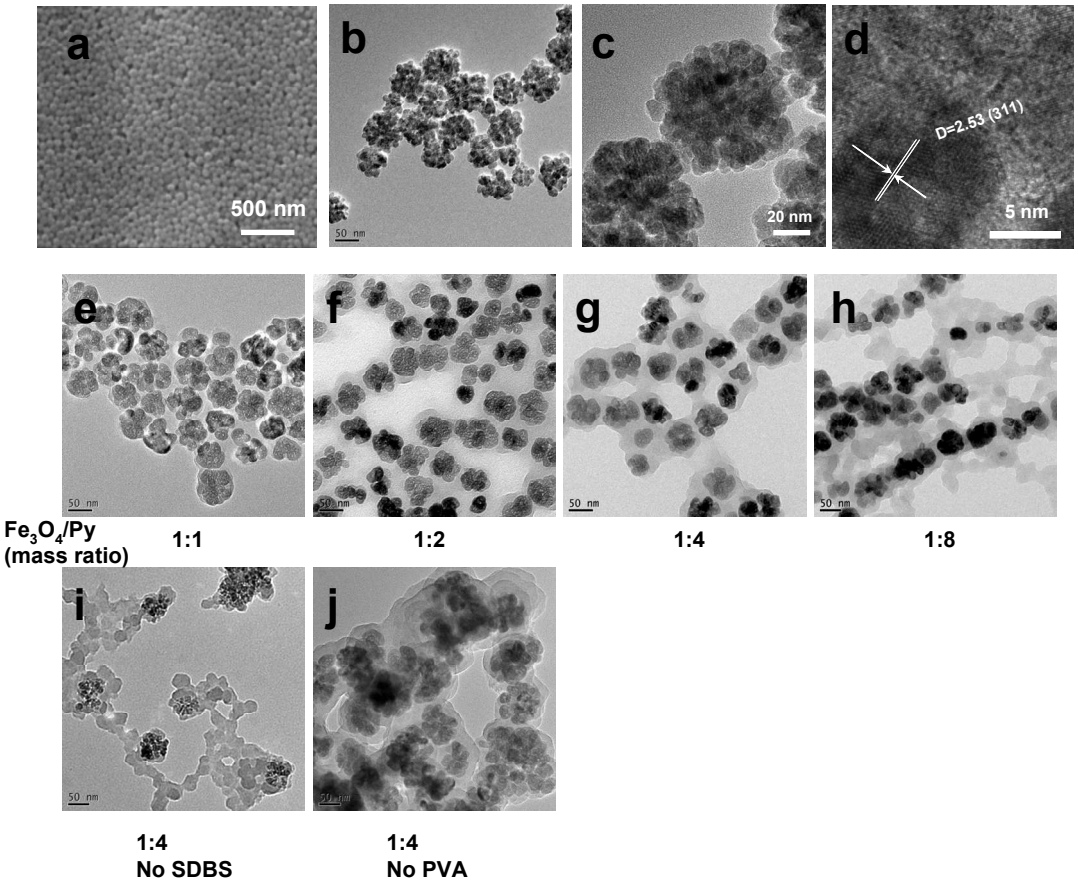

Figure S1. **(a)** A SEM image of as-synthesized Fe_3O_4 nano-clusters. The synthesis of Fe_3O_4 nano-clusters exhibited a good repeatability and the size of those nano-clusters showed a high uniformity. **(b-d)** TEM images of as-synthesized Fe_3O_4 nano-clusters, which were ~50 nm clusters of ultra-small iron oxide nanoparticles with diameters of 8-12 nm. **(e-h)** TEM images of Fe_3O_4@PPy nanocomposites synthesized with different starting Fe_3O_4 : pyrrole ratios. When the ratio of Fe_3O_4 and pyrrole monomer reached to 1:4, the obtained nanocomposites showed relatively uniform morphology. **(i&j)** TEM images of Fe_3O_4@PPy nanocomposites synthesized without addition of SDBS or PVA. The introduction of SDBS and PVA was also found to be important to control the morphology of our product.

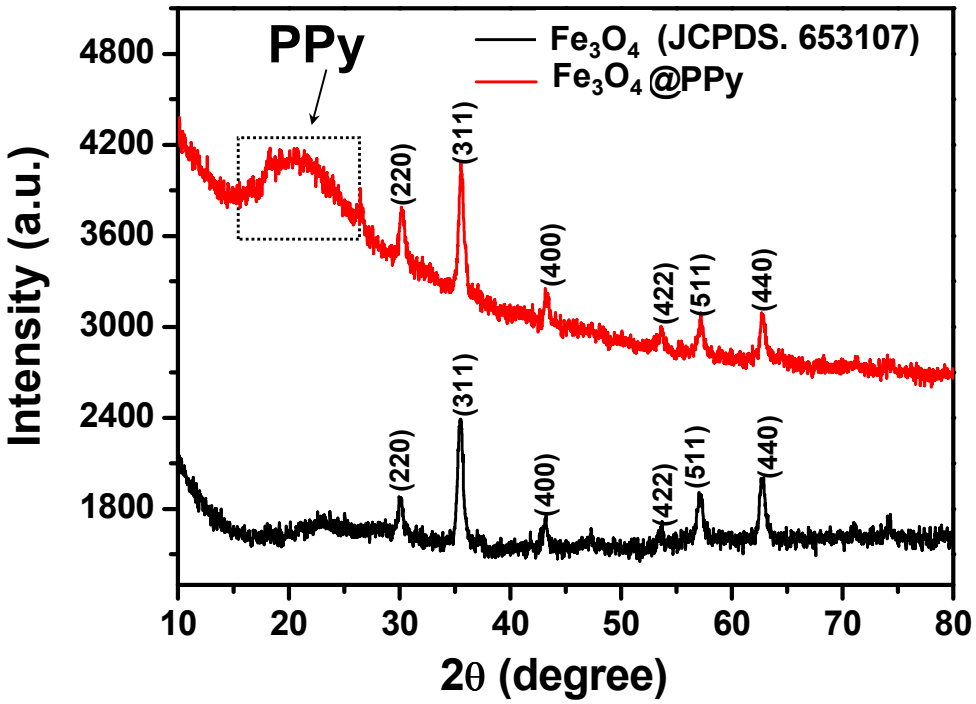

Figure S2. XRD data of Fe_3O_4 nanoclusters and Fe_3O_4@PPy nanocomposites revealed that the as-synthesized Fe_3O_4 nanoclusters were in cubic phase, and PPy polymerization on the surface of Fe_3O_4 nano-clusters would not change their crystallinity.

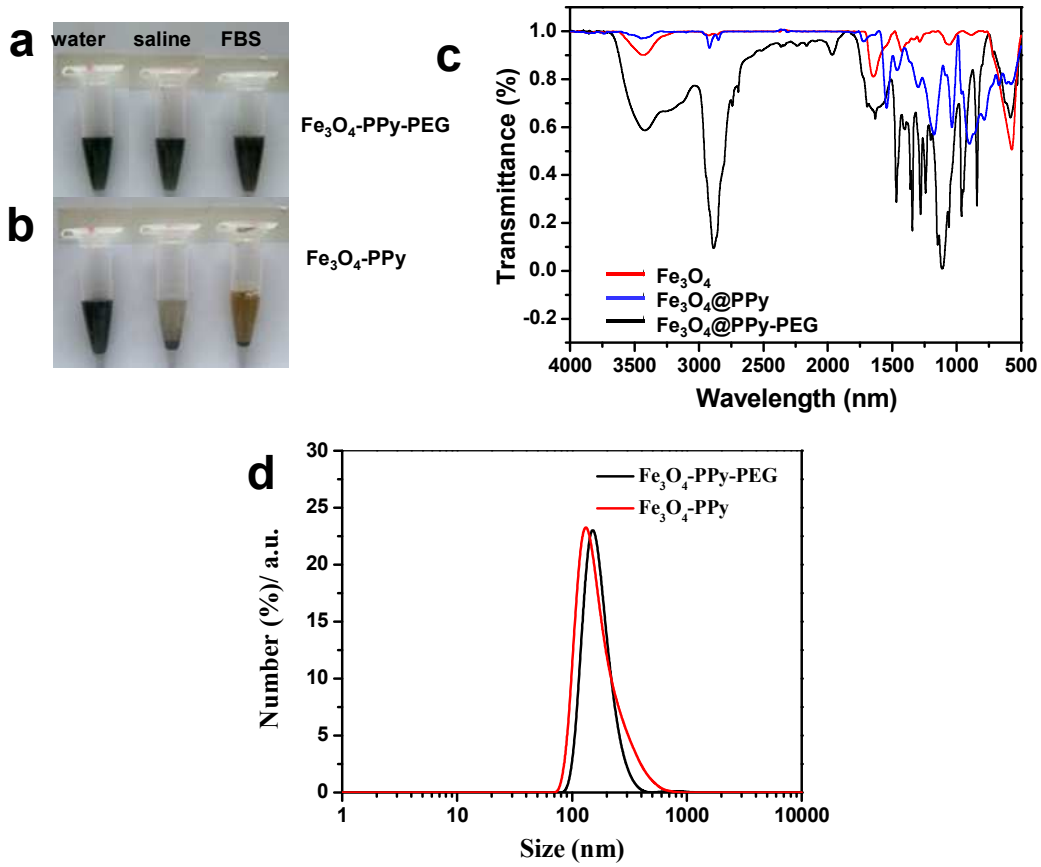

Figure S3. (a&b) Photos of Fe_3O_4@PPy nanoparticles before and after PEGylation in water, saline and serum over a week. **c)** Infrared (IR) spectra of Fe_3O_4, Fe_3O_4@PPy and Fe_3O_4@PPy-PEG. **d)** Dynamic light scattering (DLS) data of Fe_3O_4, Fe_3O_4@PPy and Fe_3O_4@PPy-PEG in water.

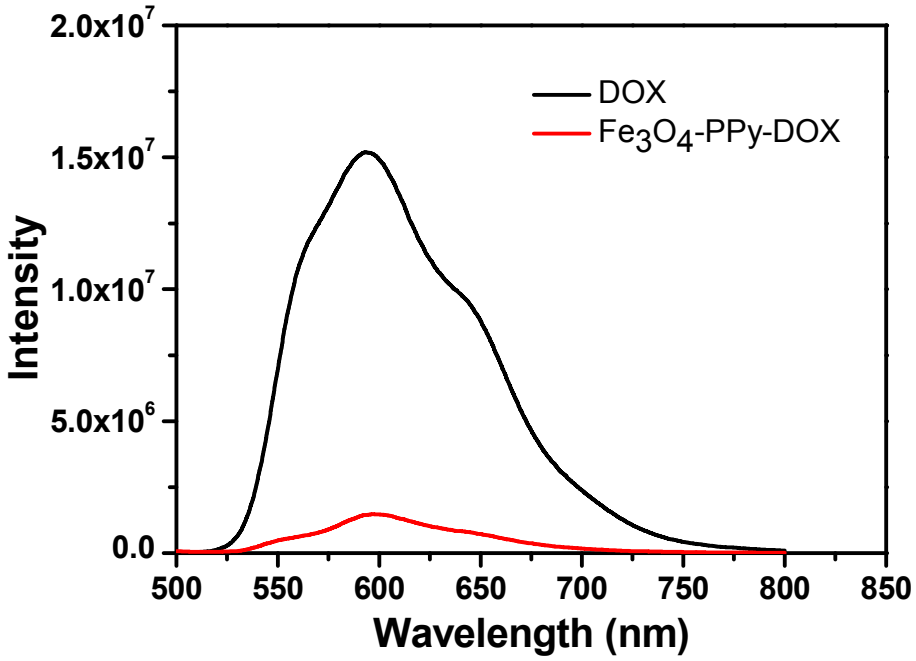

Figure S4. Fluorescence spectra of Fe_3O_4@PPy-PEG-DOX and free DOX at the same concentration of DOX. A significant DOX fluorescence quenching (~85%) effect was observed in the Fe_3O_4@PPy-PEG-DOX solution, suggesting the strong interaction between DOX and the nano-carrier.

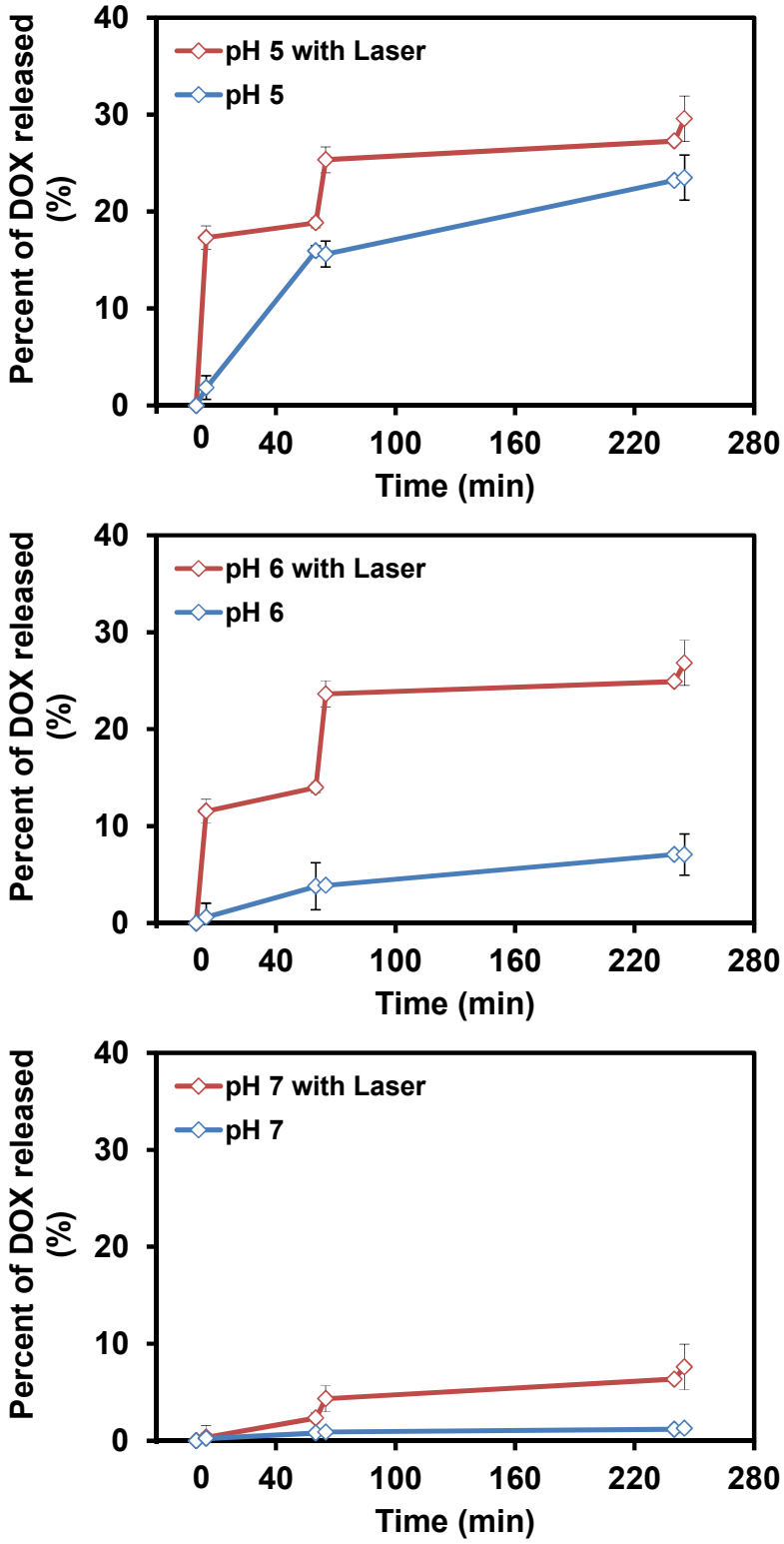

Figure S5. NIR-triggered release of DOX from Fe_3O_4@PPy-PEG nanoparticles at three pH values with or without laser irradiation.

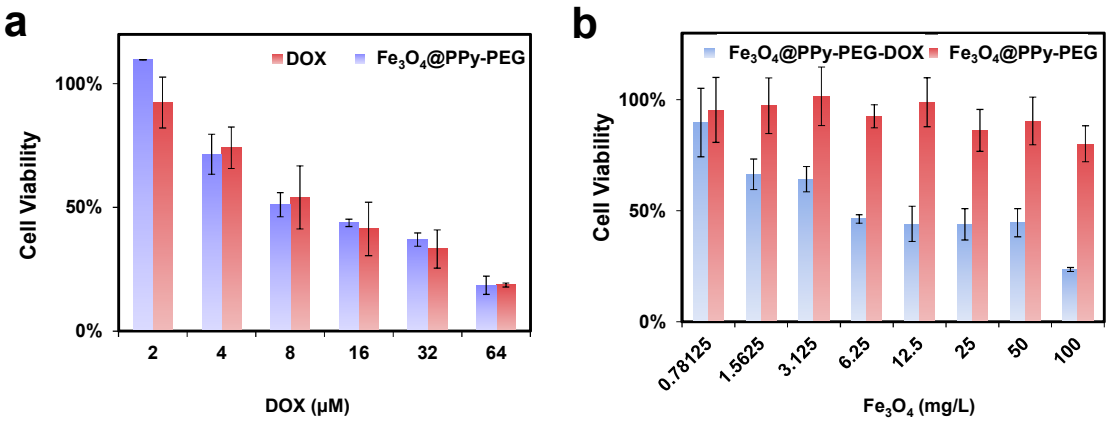

Figure S6. Relative viabilities of 4T1 cells determined 24 hours after various treatments indicated.

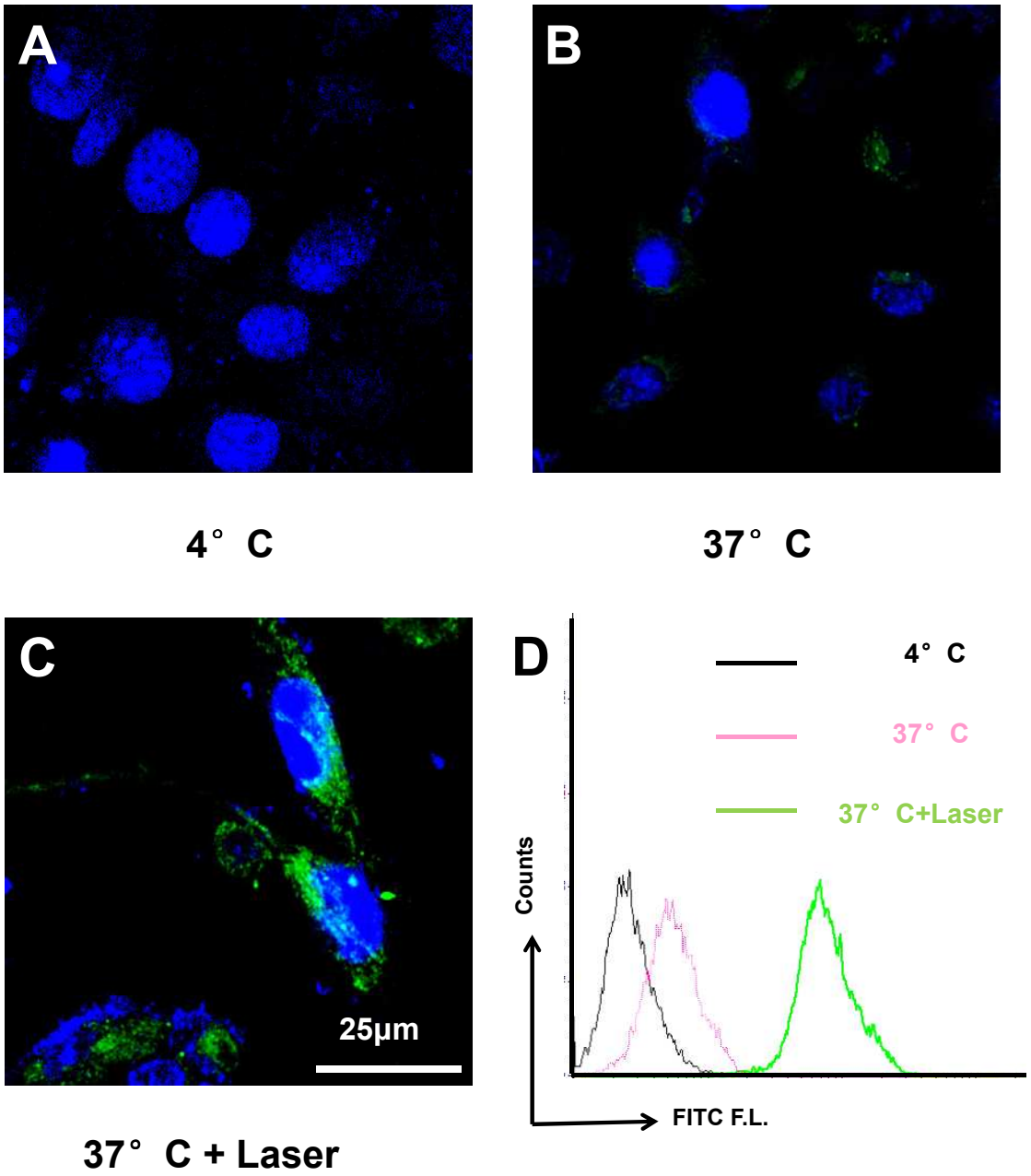

Figure S7. Photothermally enhanced cell uptake of Fe_3O_4@PPy–PEG. (a-c)Confocal fluorescence microscopy images of 4T1 cells incubated with fluorescein labeled Fe_3O_4@PPy–PEG for 30min under 4 °C in dark (a), 37 °C in dark (b), and 37 °C plus laser irradiation (350mW/cm^2) (c). Blue: DAPI; Green: fluorescein. (d) Flow cytometry measurements of cellular fluorescence in (**a-c**).

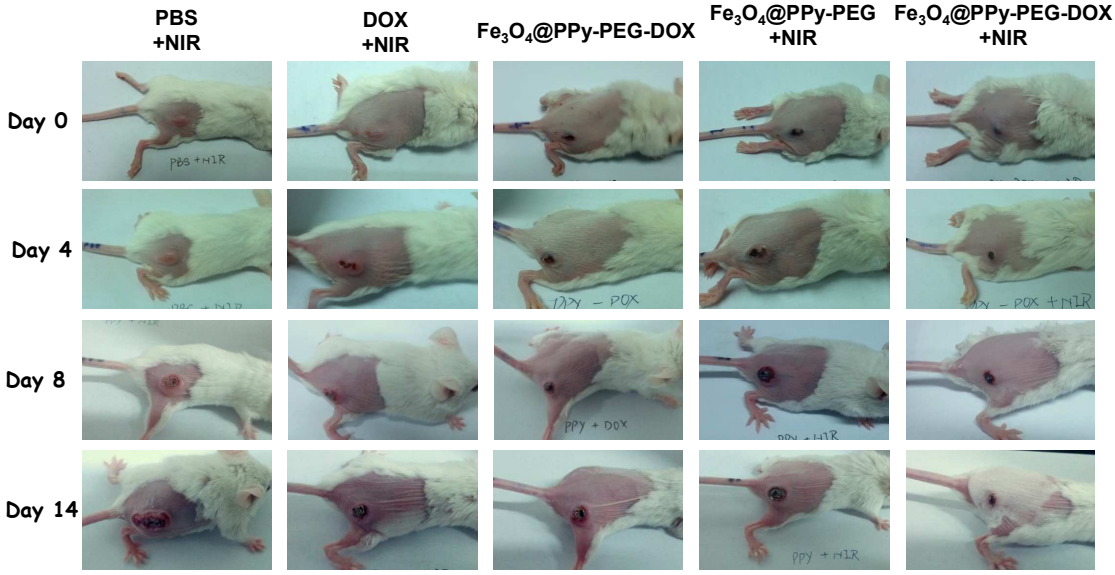

Figure S8. Photos of mice post various treatments taken at different time points.

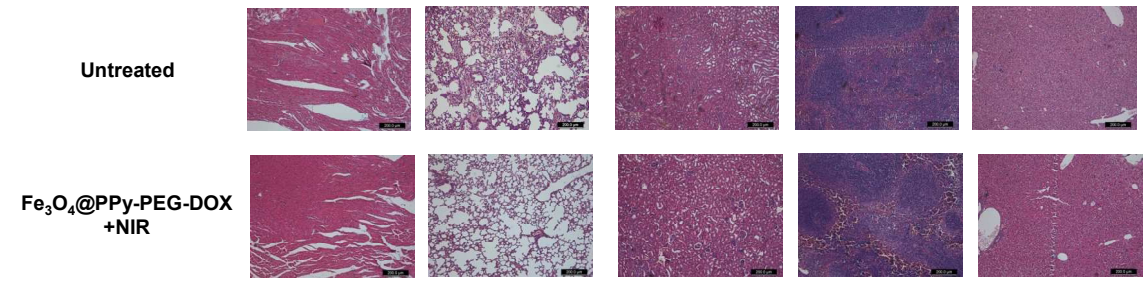

Figure S9. H&E stained micrographs of major organs collected from untreated and 'Fe_3O_4@PPy-PEG-DOX + NIR' treated mice at day 14. Scale bar = 100μm.

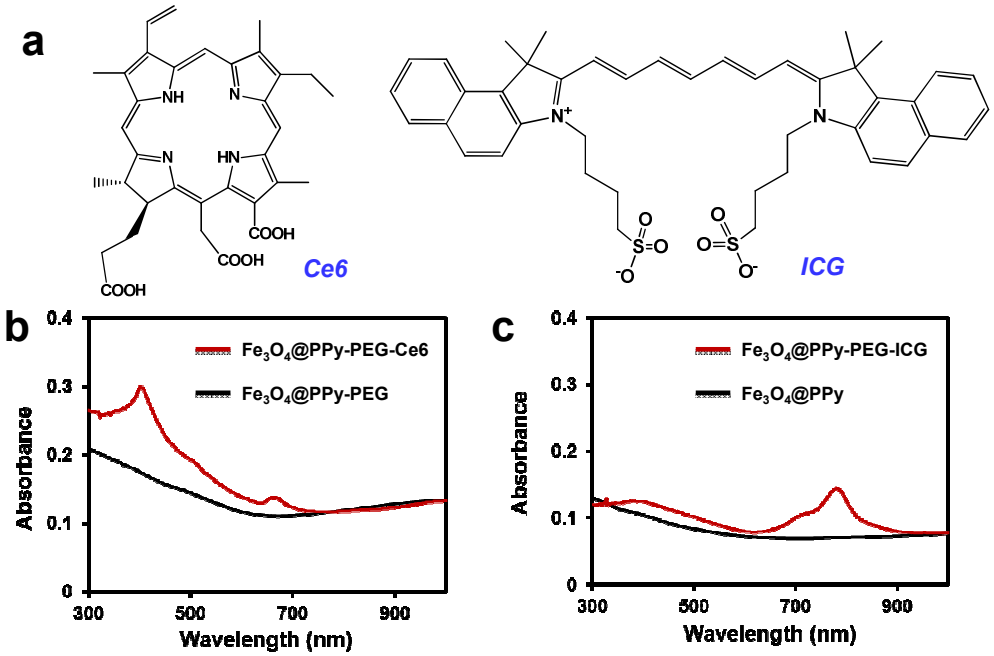

Figure S10. Ce6 and ICG loading on Fe_3O_4@PPy-PEG. **(a)** Molecular structures of Ce6 and ICG. **(b&c)** UV-VIS absorbance spectra of Fe_3O_4@PPy-PEG loaded with Ce6 **(b)** or ICG **(c)**. The loading of Ce6 and ICG on nanoparticles were conducted following the same procedure used for DOX loading except that the loading pH was 7.4 instead of 8.0.